



Radiolabeling of lacosamide using highly purified rhenium-188 as a prospective brain theranostic agent

H. A. El-Sabagh¹ · M. I. Aydia² · A. M. Amin¹ · K. M. El-Azony²

Received: 14 April 2020/Revised: 11 August 2020/Accepted: 20 August 2020/Published online: 12 October 2020

© China Science Publishing & Media Ltd. (Science Press), Shanghai Institute of Applied Physics, the Chinese Academy of Sciences, Chinese Nuclear Society and Springer Nature Singapore Pte Ltd. 2020

Abstract Rhenium-188 is prospectively effective for both diagnosis and radiotherapy as it appropriately emits gamma rays and beta particles. Lacosamide (LCM) is a newly approved antiepileptic medication for focal drug-resistant epilepsy. Rhenium-188 was separated with high elution yield and high purity using the new $^{188}\text{W}/^{188}\text{Re}$ generator based on the ZrSiW gel matrix. ^{188}Re -LCM was prepared with high radiochemical yield and high purity. Biodistribution of ^{188}Re -LCM in normal Swiss albino mice was investigated to determine its utility as a potential brain therapy agent. The $^{188}\text{W}/^{188}\text{Re}$ generator was used to obtain ^{188}Re based on the ZrSi ^{188}W gel matrix, and the chemical, radiochemical, and radionuclidic purity of the obtained ^{188}Re was determined using inductively coupled plasma optical emission spectrometry (ICP-AES), a paper chromatography technique, and high-purity germanium (HPGe) detection, respectively, to assess its validity for LCM labeling. Various factors, such as the pH, reaction time, and LCM quantity, were therefore studied in order to improve the yield and purity of ^{188}Re -LCM, as determined by various chromatographic techniques such as electrophoresis, thin layer chromatography (TLC), and high-pressure liquid chromatography (HPLC). ^{188}Re was obtained with a high elution yield ($75 \pm 3\%$) and a low ^{188}W breakthrough ($0.001 \pm 0.0001\%$). The maximum

radiochemical yield of ^{188}Re -LCM ($87.5 \pm 1.8\%$) was obtained using 50 μl LCM (4 mM), 250 μl stannous chloride (4.4 mM) at pH 4, 100 μl ^{188}Re (37 MBq), within 30 min, at room temperature ($25 \pm 3^\circ\text{C}$), as determined by TLC, electrophoresis, and HPLC techniques. Biodistribution analysis showed that ^{188}Re -LCM was primarily localized in the brain (5.1%) with a long residence time (240 min).

Keywords Lacosamide · ^{188}Re · $^{188}\text{W}/^{188}\text{Re}$ generator · Radiolabeling

1 Introduction

One of the most common radioisotopes is ^{188}Re ($T_{1/2} = 16.9$ h). It is appropriate for both radiotherapy and radiodiagnosis as it emits beta particles ($E_{\text{max}} = 2.12$ MeV) and gamma rays ($E_{\gamma} = 155$ keV, $I_{\gamma} = 15\%$). In several studies, two radionuclides have been combined for theranostic applications, such as in the case of DOTA-rituximab labeled with ^{111}In and ^{90}Y , where these isotopes are used for imaging and radiotherapy, respectively [1]. In addition to the similarity of its chemical nature to that of technetium, rhenium-188 is an effective radioisotope for in vivo applications [2–4]. ^{188}W ($T_{1/2} = 69.4$ d) is produced by double-neutron capture on natural tungsten targets, whereas ^{186}W (28.43%) occurs in low abundance; ^{186}W (n, γ) and ^{187}W have a cross section for thermal neutron capture of 38b and integral resonance of 419b [5, 6]. Similar features are exhibited by ^{187}W (n, γ) and ^{188}W , with respective values of 64 and 2760 b for the cross section for thermal capture and integrated resonance [7]. Open access to carrier-free ^{188}Re -perrhenate is a big benefit of using the $^{188}\text{W}/^{188}\text{Re}$ generator, where elution

✉ K. M. El-Azony
mmenaa_2004@yahoo.com

¹ Labeled Compound Department, Radioisotopes Production Division, Hot Laboratory Center, Atomic Energy Authority, P.O. Box 13759 Cairo, Egypt

² Radioactive Isotopes and Generators Department, Radioisotopes Production Division, Hot Laboratory Center, Atomic Energy Authority, P.O. Box 13759 Cairo, Egypt

produces about 50% ^{188}Re in 24 h. The $^{188}\text{W}/^{188}\text{Re}$ generator employs a number of matrixes, such as the ZrSiW matrix [8], which has been used as an outstanding matrix in the $^{113}\text{Sn}/^{113\text{m}}\text{In}$ generator [9]. The production of ^{188}Re requires a high-performance generator that provides great versatility in the production of a variety of therapeutic agents labeled with ^{188}Re and generators having a long shelf-life exceeding six months. A few high-flux reactors are available for producing ^{188}W [10]. The use of low-cost reusable tandem concentration units [11] offers high specific ^{188}Re volume solutions (i.e. > 700 mCi/ml for 1 Ci generator). The $^{188}\text{W}/^{188}\text{Re}$ generator is particularly important for providing a reliable source of this versatile therapeutic radioisotope, especially in developing regions where the isotope must be transported over long distances and the distribution costs are high [12].

The novel antiepileptic drug lacosamide (LCM) operates by a dual mode of action through its interactions with both the sodium voltage-gated channel and the collapsin response mediator protein 2 (CRMP2), which promote neurite outgrowth. LCM is able to reduce neuronal excitability by a voltage-gated response. Several studies point to the binding of LCM to CRMP2, as well as the ability of LCM to directly affect the function of CRMP2 [13]. CRMPs are strongly expressed in adults and in the developing nervous system [14–16]. All CRMP proteins (CRMP 1–5) are associated with the cytoskeleton [17, 18] and are important for the metastasis and invasion of cancer cells [19]. CRMP proteins have recently been implicated in a set of human cancers [20–30]. It has been reported that the neuronal autoantibody of CRMP5 is linked to patients at risk of lung carcinoma [30–32]. The role of other CRMP proteins in cancer growth still needs to be clarified. Although there is evidence that CRMP proteins play a vital role in cancer development, further exploration of the underlying mechanisms is needed.

The present work focuses on the separation of ^{188}Re based on the use of ZrSiW gel as a new $^{188}\text{W}/^{188}\text{Re}$ generator to produce ^{188}Re with high radiochemical yield and radionuclidic purity. LCM, a new antiepileptic medication, is labeled with ^{188}Re , where the ^{188}Re -LCM complex is anticipated to be relevant as a radiotheranostic agent, the action of which exploits the relationship between the presence of CRMP proteins in cancer cells and progression of the disease. The chemical structure of LCM is shown in Fig. 1.

2 Methods

2.1 Materials

All chemicals and reagents used in this work were of high purity. All experiments were carried out using doubly

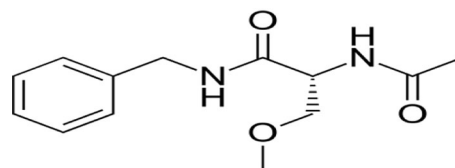


Fig. 1 2*R*)-2-(acetylamino)-*N*-benzyl-3-methoxypropanamide; lacosamide

distilled water. LCM (M.W. = 250,294 g/mol) was purchased from Aldrich Chemical Company. Stannous chloride dihydrate ($\text{SnCl}_2 \cdot 2\text{H}_2\text{O}$, M.W. = 225.64 g/mol) was purchased from Sigma Chemical Company, USA. Albino mice weighing 30–35 g were used for the experiments.

2.2 Preparation of $^{188}\text{W}/^{188}\text{Re}$ generator

Tungsten oxide (WO_3 ; $> 99.9\%$) was irradiated in the water-cooled Second Egyptian Research Reactor (ERR-2) using a thermal neutron flux of $1\text{--}5 \times 10^{14} \text{ n cm}^{-2} \text{ s}^{-1}$ for 2 d then cooled for 10 d to allow the decay of short-lived radioisotopes (ETR-2; 22 MW). The ^{188}W radioactivity was around 5 mCi (185 MBq). The irradiated WO_3 (0.56 g) was dissolved in 10 ml of 5 M NaOH and then diluted with 40 ml of distilled water to obtain 50 ml of 0.05 M ^{188}W solution. A 50 ml aliquot of 0.3 M silicate solution was prepared by dissolving 1.8 g of Na_2SiO_3 in 50 ml of water at room temperature, and the ^{188}W solution was then added to the silicate solution. The ^{188}W -silicate mixture solution was then added dropwise to 50 ml of warm 0.05 M Zr(IV) solution (0.8 g $\text{Zr OCl}_2 \cdot 8\text{H}_2\text{O}$ dissolved in 50 ml of 0.2 M HCl, at 50 °C) over 30 min, with constant stirring. The pH of the solution was adjusted from 12.8 to 8 by adding a few drops of concentrated HCl, to form a white precipitate. The gel substance was left overnight for the precipitate to settle. Thereafter, the precipitate was separated and washed with doubly distilled water until a constant pH was reached, and then dried in an electric furnace for 24 h at 50 °C [8].

2.3 Quality control of rhenium-188

2.3.1 Chemical stability

ZrSi ^{188}W gel (100 mg) was combined with 10 ml of various concentrations of HCl or NaOH and left overnight at room temperature. The ZrSi ^{188}W gel was separated by filtration and the concentrations of Zr(IV), ^{188}W (VI), and Si(IV) in the aqueous phase were determined. Inductively coupled plasma-atomic emission spectroscopy (ICP-AES) was used to determine the concentration of the studied elements (Zr, Si, and W) in the aqueous solutions after ensuring decay of the radioisotopes of tungsten.

2.3.2 Radiochemical purity

The ^{188}Re chemical species in the eluted solution were identified using ascending paper chromatography (Whatman No. 3, 15 cm long and 1 cm wide) with acetone as a developing solvent. The R_f (retardation factor) was determined as follows:

$$R_f = \frac{\text{Distance (cm) from the baseline to the peak position}}{\text{Distance (cm) from the baseline to the solvent front}}$$

2.3.3 Radionuclidic and chemical purity

The radionuclides in the eluted solution were determined immediately and after 15 days of elution to assess the ^{185}W , ^{187}W , and ^{188}W breakthrough using a HPGe detector. Direct detection of ^{185}W ($T_{1/2} = 75.1$ d) and ^{188}W ($T_{1/2} = 69.4$ d) in the presence of ^{188}Re is difficult, as they emit very low-intensity gamma lines ($E_\gamma = 125$ and 290.7 keV) ($I_\gamma = 0.019$ and 0.4% , respectively), making it difficult to distinguish ^{185}W and ^{188}W due to the high relative gamma intensity for ^{188}Re ($E_\gamma = 155$ keV, $I_\gamma = 15\%$) due to the Compton background. ^{187}W ($T_{1/2} = 23.72$ h; $E_\gamma = 134.2, 479.5,$ and 685.8 keV; $I_\gamma = 8.85, 21,$ and 27.3% , respectively) could be identified easily and instantly with the separated ^{188}Re .

2.3.4 Labeling procedure of LCM

A certain concentration of LCM was placed into a 10 ml clean penicillin vial with nitrogen-purged doubly distilled water. The vial was closed with an aluminum cap under positive pressure of nitrogen gas, and the necessary quantity of a newly prepared deoxygenated stannous chloride dihydrate solution was added. Finally, the eluted ^{188}Re (37 MBq) was added to the above mixture in order to obtain a maximum radiochemical yield at the appropriate temperature for the recommended time. The various factors affecting the radiochemical yield of ^{188}Re -LCM were investigated.

The radiochemical yield of ^{188}Re -LCM was estimated by varying the labeling factors. This was achieved by adding 250 μl of newly prepared deoxygenated stannous chloride dihydrate (25–350 μg ; 0.45–6.2 mM), 50 μl lacosamide (50 μg ; 4 mM) dissolved in water, 50 μl of different buffer solutions from pH 2 to pH 11, and varying the reaction temperature from 25 to 100 $^\circ\text{C}$ and reaction time from 5 to 60 min. The highest radiochemical yield of ^{188}Re -LCM was achieved by adding 50 μl LCM (50 μg ; 4 mM), 50 μl (pH 4) citrate buffer, 250 μl of freshly prepared stannous chloride solution (250 μg ; 4.4 mM), and ^{188}Re (100 μl , 37 MBq) at 25 $^\circ\text{C}$ within 30 min.

2.4 Radiochemical analysis

The labeling yield of the ^{188}Re -LCM complex was estimated as outlined below.

2.4.1 Electrophoresis analysis

The electrophoresis technique was used to determine the type of charge carried by the ^{188}Re -LCM complex using a Whatman No. 3 paper sheet (40 cm length \times 2.5 cm width); 5 μl of the reaction mixture was placed 8 cm away from the cathode and then spontaneously evaporated. Electrophoresis was performed with phosphate buffer (0.05 M, pH 7) as the electrolyte for 90 min at a voltage of 300 V. When the mixture reached the solvent front, the paper was removed, dried, and cut into strips, each strip being 1 cm long, and the strips were then counted in a well-type NaI (T1) crystal connected to the gamma counter. ^{188}Re -LCM remained at the spotting point and did not migrate due to the charge and ion mobility.

2.4.2 TLC analysis

The reaction mixture was filtered through a 0.22 mm Millipore filter under sufficient pressure to separate and determine the proportion of hydrolyzed ^{188}Re and stannous hydroxide colloids, as shown in the following equation:

$$\text{Colloid \%} = \frac{\text{Activity before filtration} - \text{Activity after filtration}}{\text{Total activity}} \times 100$$

Secondly, the TLC silica gel sheets were marked with a line 2 cm from the bottom using a blunt pencil and cut into segments of 1–13 cm each. After the filtration process, 5 μl of the filtered solution was spotted on the sheet and a saline solution of 0.9% NaCl was used for development in a closed jar. The sheet was removed, dried, and cut into small pieces, each piece having a width of 1 cm, and counted in a gamma counter. $^{188}\text{ReO}_4^-$ moved with the solvent front ($R_F = 1$), while the ^{188}Re -LCM complex remained at the baseline ($R_F = 0$). The radiochemical yield of ^{188}Re -LCM was calculated as follows:

$$\%^{188}\text{ReO}_4 = \frac{^{188}\text{ReO}_4 \text{ activity}}{\text{Total activity}} \times 100$$

$$\text{Radiochemical yield, \%} = 100 - (\% \text{ colloid} + \% ^{188}\text{ReO}_4)$$

2.5 Determination of partition coefficient

The partition coefficient was determined to evaluate the ability of radiopharmaceuticals to pass through the blood–

brain barrier (BBB) by in vitro screening. This experiment was carried out by mixing ^{188}Re -LCM in a centrifuge tube with the same amounts of phosphate buffer and 1-octanol (0.025 M at pH 7.4). The mixture was shaken at room temperature for 1 min and then centrifuged at 5000 rpm for 5 min. A 100 μl aliquot from each phase was drawn into test tubes and counted. The partition coefficient was identified as the ratio of the organic to aqueous phase. Measurements were carried out in triplicate according to the following equation; the partition coefficient is expressed as $\log p$ [33].

$$\log p_{\text{oct/buf}} = \frac{[\text{Solute}]_{\text{octanol}}}{[\text{Solute}]_{\text{phosphate buffer}}}$$

2.6 HPLC analysis

The radiochemical purity of ^{188}Re -LCM was determined by direct injection of 5–10 μl of the reaction solution into the chromatographic column (RP18—250 \times 4 mm, 5 μm , Lischrosorb) using the HPLC Shimadzu instrument consisting of LC-9A pumps with a Rheohydrion injector and UV detector (SPD-6A). Detection was performed at 210 nm. Sodium dihydrogenphosphate monohydrate at pH 3 in acetonitrile (700:300 v/v) was used at a flow rate of 1.0 ml/min, with a column temperature of 40 $^{\circ}\text{C}$ [34]. A fraction collector was used to collect the labeled complex, and the activity of the complex was measured using a NaI (TI) well-type crystal connected to a single-channel analyzer.

2.7 Molecular mass analysis

The molecular mass of Re-LCM was measured using a Shimadzu GCMS-QP-1000EX mass spectrometer (Research and Development Center for Drug Discovery, Ain Shams University, Cairo, Egypt). The optimum conditions for preparing Re-LCM were achieved by using inactive perrhenate (ReO_4^-) instead of $^{188}\text{ReO}_4^-$ with the same molar ratio of LCM to perrhenate to stannous chloride (1:1:5) at pH 4. The reaction was performed for 30 min at room temperature.

2.8 Biodistribution studies

The animal research was carried out under the supervision of the governmental research authority. The mice comprised one group of normal albino mice. The experiment was carried out by diluting the purified ^{188}Re -LCM neutral solution with 1 ml of saline to filter the solution using a 0.22 μm Millipore filter, after which the animals were injected with the solution for the biodistribution

study. Healthy albino mice, each weighing approximately 30–35 g, were injected in the tail vein using 200 μl of the solution with a specific activity of 30 MBq ^{188}Re per 0.002 mmol LCM. The mice were kept in a metabolic cage on ordinary diet and then killed 10, 60, 120, and 240 min after injection. Fresh blood, bone, and muscle samples were collected in pre-weighed vials and counted. The various organs were separated and counted. The mean percentage of the delivered dose per organ was calculated. Blood, bone, and muscles were assumed to be 7, 10, and 40% of the total body weight, respectively [35].

3 Results and discussion

3.1 $^{188}\text{W}/^{188}\text{Re}$ generator

The $\text{ZrSi}^{188}\text{W}$ gel was prepared for the $^{188}\text{W}/^{188}\text{Re}$ generator with a high content of tungsten (393.3 mg W/g gel) [8]. ^{188}Re was eluted using a saline solution at a flow rate of 0.5 ml/min (0.9% NaCl); substantial removal (> 90%) was obtained in the first 4 ml. The elution yield of ^{188}Re and the ^{188}W breakthrough were found to be 75 ± 3 and $10^{-3} \pm 2 \times 10^{-4} \%$, respectively.

The ascending paper chromatography technique employing a Whatman No. 3 paper and acetone as a developing solvent was used to determine the purity of ^{188}Re . Figure 2a shows a single peak corresponding to $98 \pm 0.06\%$ radiochemical purity at $R_f \sim 1$, related to $^{188}\text{ReO}_4^-$ [8].

Gamma ray spectrometry and radioactive decay measurements were performed using an HPGe detector linked to a multi-channel analyzer to confirm the separation of ^{188}Re , free of any radionuclides, as shown in Fig. 2b.

3.2 Preparation of ^{188}Re -LCM

3.2.1 Effect of stannous chloride concentration

Figure 3a shows the effect of the amount of stannous chloride on the radiochemical yield of ^{188}Re -LCM. The labeling yield of ^{188}Re -LCM increased from 12.3 ± 0.2 to $87.5 \pm 1.8\%$ when the quantity of stannous chloride was increased from 25 to 250 μg . Stannous chloride exceeding 250 μg led to a decrease in the ^{188}Re -LCM yield from 57.7 ± 0.6 at 300 μg to $39.9 \pm 0.4\%$ at 350 μg . The decrease in the ^{188}Re -LCM yield with low amounts of stannous chloride may be due to insufficient stannous chloride to reduce all the rhenium(VII) (ReO_4^-) to the lower oxidation states [36, 37]. Most of the ligand molecules were involved in complex formation; thus, perrhenate was reduced to insoluble rhenium(IV) ($\text{ReO}_2 \cdot x\text{H}_2\text{O}$) in the absence of the ligand at high concentrations of stannous

Fig. 3 a The radiochemical yield of ^{188}Re -lacosamide as a function of amounts of stannous chloride [100 μL (37 MBq) $^{188}\text{ReO}_4^-$, 50 μL of lacosamide (4 mM) in distilled water, 50 μL phosphate buffer (pH 4), 250 μL (x mM) stannous chloride] at 25 $^\circ\text{C}$ within 30 min reaction time. **b** The radiochemical yield of ^{188}Re -lacosamide as a function of pH value [100 μL (37 MBq) $^{188}\text{ReO}_4^-$, 50 μL of lacosamide (4 mM) in distilled water, 50 μL Phosphate buffer variable pH, 250 μL (4.4 mM) stannous chloride] at 25 $^\circ\text{C}$ within 30 min. **c** The radiochemical yield of ^{188}Re -lacosamide as a function of reaction temperature [100 μL (37 M Bq) $^{188}\text{ReO}_4^-$, 50 μL of lacosamide (4 mM) in distilled water, 50 μL phosphate buffer (pH 4), 250 μL stannous chloride (4.4 mM)] at 30 min and different reaction temperatures. **d** The radiochemical yield of ^{188}Re -lacosamide as a function of reaction time [100 μL (37 MBq) $^{188}\text{ReO}_4^-$, 50 μL lacosamide (4 mM) in distilled water, 50 μL phosphate buffer (pH 4), 250 μL stannous chloride (4.4 mM)] at 25 $^\circ\text{C}$ and different reaction times

chloride [38]. In addition, the reduction reaction rate increased to produce a colloid at high concentration of Sn(II), where tin appears to be more competitive with regard to the complexation reaction, thereby reducing the labeling yield of ^{188}Re -LCM.

3.3 Effect of pH

Figure 3b presents the results obtained when ^{188}Re -LCM was prepared by varying the pH of the reaction medium. In acidic medium (pH = 2), hydrated $^{188}\text{ReO}_2$ may be formed [39], which reacts with other reagents, such

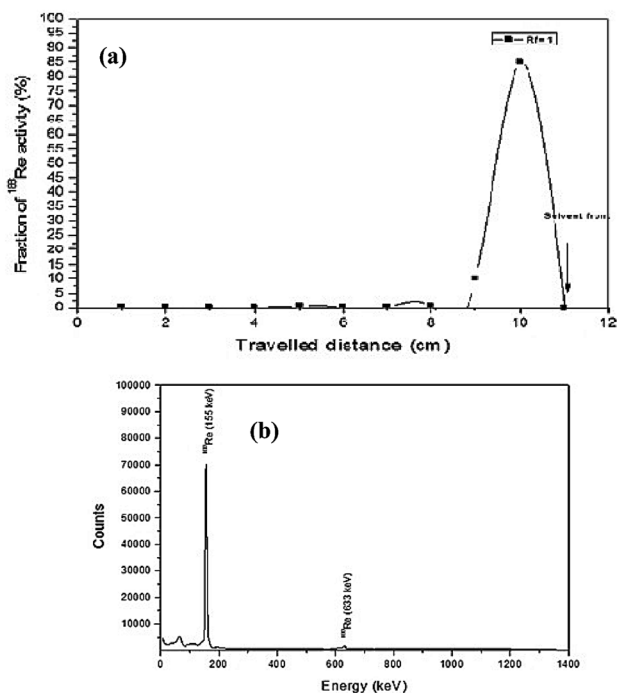
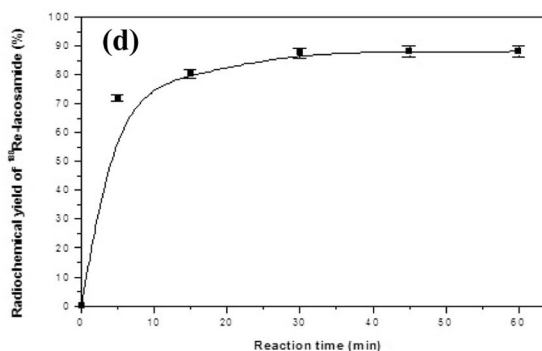
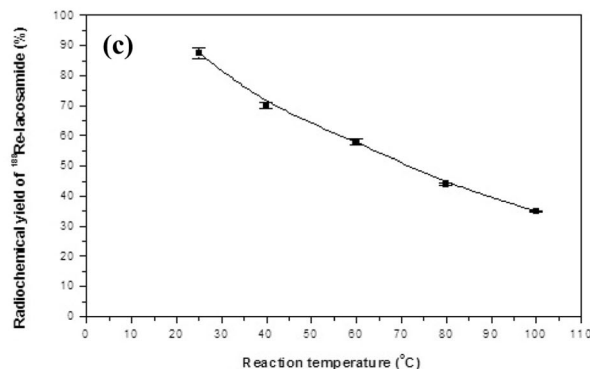
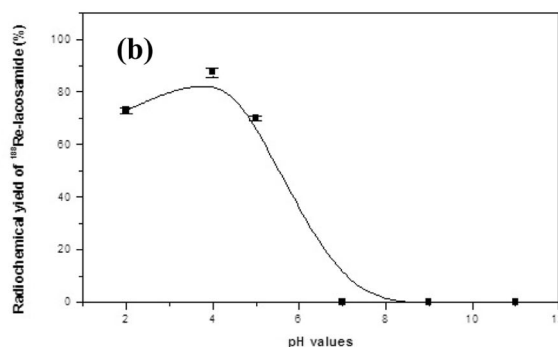
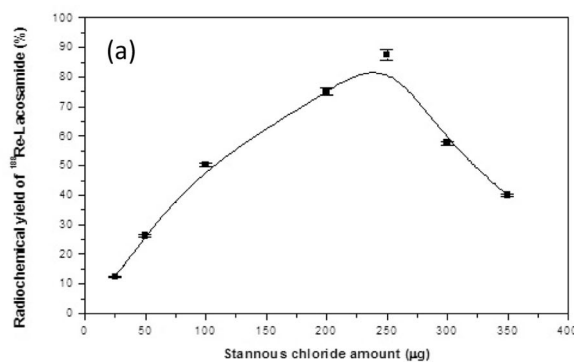


Fig. 2 a Radiochromatogram of the eluted ^{188}Re , using Whatman No.3 ascending paper chromatographic method and acetone as a developing solvent. **b** Gamma ray spectrum of the ^{188}Re eluate

as SnO, to form a $^{188}\text{ReO}_2$ complex during the perrhenate reduction reactions using stannous chloride [40]; this reduced the radiochemical yield of the ^{188}Re -LCM complex to $73 \pm 1.1\%$. Upon increasing the pH from 2 to 4, the radiochemical yield of ^{188}Re -LCM reached a maximum value of $87.5 \pm 1.8\%$. At pH greater than 8, the yield of ^{188}Re -LCM dropped dramatically, which may be due to stannous hydroxide ($\text{Sn}(\text{OH})_3$) formation [36, 37]. Moreover, the low yield of ^{188}Re -LCM may be due to the fact that LCM is more readily hydrolyzed in alkaline solutions compared to acidic solutions [41].

3.4 Effect of reaction temperature

The highest labeling yield of ^{188}Re -LCM ($87.5 \pm 1.8\%$) was obtained at room temperature ($25 \pm 3^\circ\text{C}$), followed by a gradual decrease to $35 \pm 0.2\%$ when the temperature of the reaction was increased to 100°C (Fig. 3c). The results demonstrate that room temperature ($25 \pm 3^\circ\text{C}$) is the most appropriate temperature for formation of the ^{188}Re -LCM complex. Although LCM is stable and does not decompose up to 70°C for 7 d when it is exposed to dry heat [41], the radiochemical yield of ^{188}Re -LCM decreased when the temperature was raised. This may be due to disintegration of the ^{188}Re -LCM complex, without any effect on LCM up to 70°C .

3.5 Effect of reaction time

The influence of the reaction time (5, 15, 30, 45, and 60 min) on the labeling yield of ^{188}Re -LCM is shown in Fig. 3d. The yield of ^{188}Re -LCM increased from 72.1 ± 1.1 to $87.5 \pm 1.8\%$ and achieved equilibrium when the reaction time was increased from 5 to 30 min at room temperature.

3.6 Fragmentation of Re-LCM

Figure 4a shows the full-scan mass spectrum of Re-LCM in the range of 100–800 m/z . The MS data for Re-LCM were acquired in positive ion mode and displayed peaks at m/z values of 456/453, corresponding to the $[\text{M} + \text{H}]^+$ ions. The fragmentation of Re-LCM produced an ion peak at m/z 439 due to the loss of H_2O from the parent ion. The removal of a methoxyl and water group from the parent ion formed the fragment ion at m/z 408, which was further fragmented to generate the ion at m/z 256.

3.7 Reaction mechanism

Mass spectral analysis indicated that Re-LCM was successfully formed on the basis of the molecular mass of

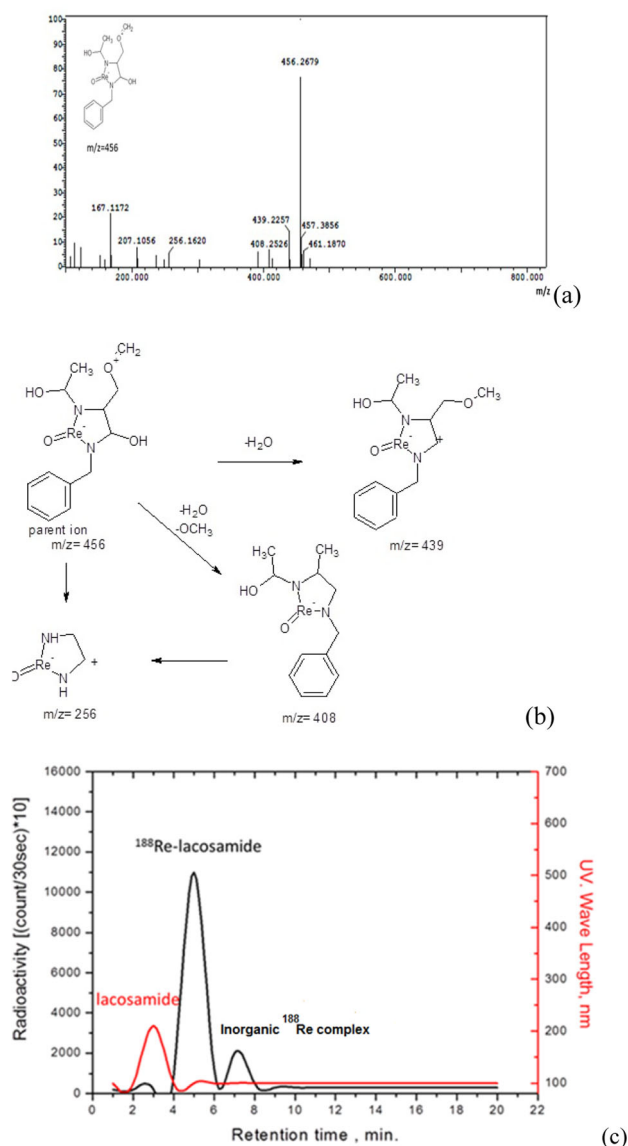
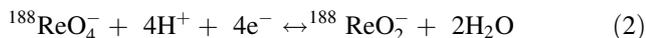


Fig. 4 a Mass spectra of Lacosamide-Re ($m/z = 456$) and its product ion ($m/z = 453$). b The proposed fragmentation pathway and product ion structures based on the interpretation of the mass spectrum of lacosamide-Re. c High-performance liquid chromatography elution profile of ^{188}Re , lacosamide and ^{188}Re -lacosamide separated on reversed phase column (RP18-250 mm \times 4 mm, 5 μm , Lichrosorb) at a flow rate of 1 ml/min

the parent ion ($m/z = 456$) and confirmed that one molecule of LCM binds with the Re(III) oxo core to form a complex. Herein, Re-LCM was prepared using a 1:1:5 molar ratio of LCM/perrhenate/stannous chloride at pH 4, at room temperature, within 30 min. This ratio was used in order to reduce Re from (VII) to (III), to facilitate reaction between one molecule of LCM and the Re(III) oxo core to form the suggested complex (Fig. 4b) according to the following equations:



3.8 Stability of ^{188}Re -LCM

The stability of ^{188}Re -LCM was studied at room temperature (25 ± 3 °C) to determine the appropriate time for injection to avoid the formation of unwanted products, because these unwanted radioactive products can accumulate in non-target organs. Table 1 shows the stability of ^{188}Re -LCM up to 24 h.

3.9 In vitro stability of ^{188}Re -LCM in serum

The in vitro stability of the ^{188}Re -LCM complex was also studied in blood serum. In this experiment, 5 ml of blood was taken and centrifuged for 5 min at 3000 rpm; the blood serum was then separated from the blood cells. A 1.5 ml aliquot of serum was taken in a clean vial and 0.5 ml of ^{188}Re -LCM was added. The vial was incubated at 37 °C, and the radiochemical purity of the labeled complex was checked at various time intervals (1–8 h), as shown in Table 2.

3.10 Lipophilicity

The ^{188}Re -LCM partition coefficient was found to be 2.31 ± 0.02 , which indicates that the brain–blood barrier (BBB) could be easily crossed by the target.

3.11 HPLC analyses

Figure 4c displays the UV absorbance of LCM and the radiochromatogram of ^{188}Re -LCM. The species in the radiolabeling reaction mixture were elucidated separately at specific retention times (R_t). LCM, ^{188}Re -LCM, and the inorganic ^{188}Re -complex were separated at retention times

Table 1 Stability of ^{188}Re - LCM

Time post-labeling (h)	^{188}Re -Lacosamide, %at room temperature Mean \pm S.D.
1	87.5 \pm 0.7
2	85.1 \pm 1.3
4	83.8 \pm 0.9
8	82.4 \pm 1.6
12	82.3 \pm 1.1
24	82.0 \pm 0.7

Mean \pm S.D. (mean of three experiments)

Table 2 The in vitro stability of ^{188}Re -LCM in serum

Time post-labeling (h)	^{188}Re -Lacosamide, % in serum at 37 °C Mean \pm S.D.
1	87.5 \pm 0.9
2	87.4 \pm 0.5
4	87.1 \pm 1.2
8	86.7 \pm 0.7

of 3, 5, and 7 min, respectively. The retention time of the inorganic ^{188}Re -complex on the RP-18 column is longer than that of ^{188}Re -LCM, which may be because the molecular weight of the inorganic ^{188}Re -complex is greater than the molecular weight of ^{188}Re -LCM. The inorganic ^{188}Re -complex may also interfere with the ^{188}Re -LCM in vivo study. Thus, HPLC must be used to separate the undesired inorganic ^{188}Re -complex from ^{188}Re -LCM. The fractions containing the ^{188}Re -LCM complex were collected and evaporated to remove the solvent under vacuum (reduced pressure). The residue was redissolved in physiological saline and filtered by using a 0.22 μm Millipore filter for sterilization. The resulting ^{188}Re -LCM preparation was suitable for the biodistribution studies.

3.12 Biodistribution study

The in vivo behavior of ^{188}Re -LCM was determined in mice at 10, 60, 120, and 240 min after intravenous injection. Table 3 presents the bio-evolution of the radiolabeled complex in the most relevant organs. Bio-evolution of ^{188}Re -LCM in normal mice showed that the complex had high initial blood, muscle, and bone uptake at 10 min post-injection. The clearance of ^{188}Re -LCM from the blood was high, as the proportion reached 6.1% at 240 min after injection, which may be due to low plasma protein binding of ^{188}Re -LCM. The present biodistribution data are consistent with the data presented by De Biase et al. [42] and Wong and Sountain [43] who reported low binding of plasma protein with LCM. ^{188}Re -LCM is capable of crossing the blood brain barrier, resulting in significant initial brain uptake (1.9% at 10 min), maximum brain localization (5.2% at 120 min), and good retention (4.3% at 240 min post-injection) in mice.

The maximum brain localization of ^{188}Re -LCM is higher than that of the commercially available $^{99\text{m}}\text{Tc}$ -HMPAO and $^{99\text{m}}\text{Tc}$ -ECD, and the retention time is better than that of the recently research-proven brain imaging radiopharmaceuticals $^{99\text{m}}\text{Tc}$ -trazadone and $^{99\text{m}}\text{Tc}$ -ropinir-ole [44–47].

^{188}Re -LCM was removed from circulation mainly through the urine (approximately 37.1% at 240 min after

Table 3 Biodistribution of ^{188}Re -LCM in normal mice

Organs or body fluids	Time post-injection (min)			
	10	60	120	240
Brain	1.9 ± 0.5	3.8 ± 0.3	5.6 ± 0.2	4.3 ± 0.1
Blood	20.3 ± 1.0	13.9 ± 0.7	9.0 ± 0.6	6.1 ± 0.2
Liver	15.8 ± 0.8	8.3 ± 0.6	7.3 ± 0.4	7.5 ± 0.3
Intestine	10.9 ± 0.4	14.2 ± 0.9	11.4 ± 1.1	9.2 ± 1.3
Stomach	5.1 ± 0.4	7.0 ± 0.7	10.3 ± 1.0	9.0 ± 0.5
Lungs	1.2 ± 0.2	1.4 ± 0.2	1.5 ± 0.1	1.7 ± 0.1
Heart	1.3 ± 0.1	1.4 ± 0.1	0.8 ± 0.1	0.6 ± 0.1
Kidneys	13.7 ± 0.3	10.3 ± 0.4	11.6 ± 0.4	13.1 ± 0.2
Spleen	1.1 ± 0.1	0.9 ± 0.1	0.8 ± 0.1	0.3 ± 0.1
Muscles	5.1 ± 0.3	4.9 ± 0.4	3.7 ± 0.2	3.0 ± 0.2
Bones	3.3 ± 0.3	3.9 ± 0.2	5.1 ± 0.1	5.7 ± 0.1
Thyroid	0.3 ± 0.1	0.7 ± 0.1	0.9 ± 0.1	1.1 ± 0.1
Urine	18.0 ± 0.8	28.3 ± 0.6	30.2 ± 1.2	37.1 ± 2.4
Brain ^a	4.8 ± 0.5	9.5 ± 0.3	14.0 ± 0.2	10.8 ± 0.1
Blood ^b	7.3 ± 1.0	5.0 ± 0.7	3.2 ± 0.6	2.1 ± 0.2
(Br/BI) ^c	0.66	1.9	4.38	5.1

^a%Injected dose/g tissue^bBr Brain, BI Blood^cBr/BI: target/non-target

^{188}Re -LCM injection) [42, 43, 48]. With respect to the radioactivity delivered to the brain per gram tissue in the blood (target to non-target ratio), it was found that the ratio increased as time passed, reaching a maximum value of 5.1 at 240 min after injection. ^{188}Re -LCM was mainly removed from the circulation, with low wash out from brain tissue, indicating the ability and efficiency of ^{188}Re -LCM to localize in the brain due to its binding with CRMP2, as well as its ability to directly impact the role of CRMP2 [13]. A site of interaction between LCM and its target CRMP2 protein has not been identified; molecular modeling revealed five pockets capable of binding LCM [49]. The phenyl ring of LCM is ensconced in a cavity of CRMP2; therefore, ^{188}Re incorporation did not affect the pharmacological properties of LCM.

4 Conclusion

^{188}Re -LCM as a new radiolabeled agent for CRMP2 targeted cancer theranostics could be produced in a yield of $87.5 \pm 1.8\%$ under the optimal reaction conditions using 50 μl LCM (4 mM), 250 μl stannous chloride (4.4 mM), at pH 4, with 100 μl ^{188}Re (37 MBq), at room temperature, within 30 min. This agent is stable both in vitro and in vivo. Biodistribution study of ^{188}Re -LCM in normal mice and calculation of the target to non-target ratio (T/NT) showed that both high uptake and long retention in the

brain were achieved. Further studies on the potential of ^{188}Re -LCM as a therapeutic agent for treating brain cancer cells are warranted in the future.

Compliance with ethical standards

Ethical approval All international, national, and/or institutional guidelines applicable were pursued in the care and use of animals.

References

1. N. Gholipour, A.R. Jalilian, A. Khalaj et al., Preparation and radiolabeling of a lyophilized (kit) formulation of DOTA-rituximab with Y and In for domestic radioimmunotherapy and radioscinigraphy of Non-Hodgkin's Lymphoma. *DARU J. Pharm. Sci.* **22**(1), 58 (2014). <https://doi.org/10.1186/2008-2231-22-58>
2. F.-Y.J. Huang, G.-Y. Guo, W.-Y. Lin et al., Investigation of the local delivery of an intelligent chitosan-based ^{188}Re thermosensitive in situ-forming hydrogel in an orthotopic hepatoma-bearing rat model. *J. Radioanal. Nucl. Chem.* **299**(1), 31–40 (2014). <https://doi.org/10.1007/s10967-013-2742-1>
3. S. Pervez, A. Mushtaq, M. Arif, Z.H. Chohan, ^{188}Re -EDTMP: a potential therapeutic bone agent. *J. Radioanal. Nucl. Chem.* **257**(2), 417–420 (2003). <https://doi.org/10.1023/A:1024712719553>
4. M.Y. Nassar, M.T. El-Kolaly, M.R.H. Mahran, Synthesis of a ^{188}Re -DTPMP complex using carrier-free ^{188}Re and study of its stability. *J. Radioanal. Nucl. Chem.* **287**(3), 779–785 (2011). <https://doi.org/10.1007/s10967-010-0933-6>
5. E.K. Elmaghraby, Investigation of epi-thermal shape-parameter needed for precision analysis of activation. *Eur. Phys. J. Plus.*

- 132(249), 1–34 (2017). <https://doi.org/10.1140/epjp/i2017-11516-7>
6. S. Pervez, A. Mushtaq, M. Arif, Preparation of ^{188}Re -labeled hydroxyapatite for radiosynovectomy. *J. Radioanal. Nucl. Chem.* **254**(2), 383–385 (2002). <https://doi.org/10.1023/A:1021604806814>
 7. S.F. Mughabghab, Neutron resonance parameters and thermal cross section. Neutron Cross Sections. Academic Press, Orlando (printed book) (1984). <https://www.elsevier.com/books/neutron-cross-sections/mughabghab/978-0-12-509711-6>
 8. M.I. Aydia, H. El-Said, A.A. El-Sadek et al., Preparation and characterization of zirconium silico- ^{188}W -tungstate as a base material for $^{188}\text{W}/^{188}\text{Re}$ generator. *Appl. Radiat. Isot.* **142**, 203–210 (2018). <https://doi.org/10.1016/j.apradiso.2018.09.026>
 9. H. El-Said, A.A. El-Sadek, M.I. Aydia et al., Zirconium silico-tungstate matrix as a prospective sorbent material for the preparation of $^{113}\text{Sn}/^{113\text{m}}\text{In}$ generator. *J. Radioanal. Nucl. Chem.* **317**, 1341–1347 (2018). <https://doi.org/10.1007/s10967-018-5991-1>
 10. F.F. Knapp Jr., A.P. Callahan, A.L. Beets et al., Processing of reactor-produced tungsten-188 for fabrication of clinical-scale alumina based tungsten-188/rhenium-188 generators. *Appl. Radiat. Isot.* **45**(12), 1123–1128 (1994). [https://doi.org/10.1016/0969-8043\(94\)90026-4](https://doi.org/10.1016/0969-8043(94)90026-4)
 11. F. F. Knapp Jr, A. L. Beets, S. Mirzadeh, et al., Use of a new tandem cation/anion exchange system with clinical-scale generators provides high specific volume solutions of technetium-99/ and rhenium-188. In, IAEA -TECDOC-1029, p 419(1998) https://inis.iaea.org/search/search.aspx?orig_q=RN:29061149
 12. F.F. Knapp Jr, A.L. Beets, J. Pinked, et al., Rhenium radioisotopes for therapeutic radiopharmaceutical development. IAEA-SR-209/L11, p 156 (1999). https://inis.iaea.org/Collection/NCLCollectionStore/_Public/29/067/29067622.pdf?r=1
 13. S.M. Wilson, R. Khanna, Specific binding of lacosamide to collapsin response mediator protein 2 (CRMP2) and direct impairment of its canonical function: implications for the therapeutic potential of lacosamide. *Mol. Neurobiol.* **51**(2), 599–609 (2015). <https://doi.org/10.1007/s12035-014-8775-9>
 14. J.E. Minturn, H.J. Fryer, D.H. Geschwind et al., TOAD-64, a gene expressed early in neuronal differentiation in the rat, is related to unc-33, a *C. elegans* gene involved in axon outgrowth. *J. Neurosci.* **15**(10), 6757–6766 (1995). <https://doi.org/10.1523/JNEUROSCI.15-10-06757.1995>
 15. M. Fukada, I. Watakabe, J. Yuasa-Kawada et al., Molecular characterization of CRMP5, a novel member of the collapsin response mediator protein family. *J. Biol. Chem.* **275**(48), 37957–37965 (2000). <https://doi.org/10.1074/jbc.M003277200>
 16. J. Yuasa-Kawada, R. Suzuki, F. Kano et al., Axonal morphogenesis controlled by antagonistic roles of two CRMP subtypes in microtubule organization. *Eur. J. Neurosci.* **17**(11), 2329–2343 (2003). <https://doi.org/10.1046/j.1460-9568.2003.02664.x>
 17. Y. Fukata, T.J. Itoh, T. Kimura et al., CRMP-2 binds to tubulin heterodimers to promote microtubule assembly. *Nat. Cell Biol.* **4**(8), 583–591 (2002). <https://doi.org/10.1038/ncb825>
 18. S. Brot, V. Rogemond, V. Perrot et al., CRMP5 interacts with tubulin to inhibit neurite outgrowth, thereby modulating the function of CRMP2. *J. Neurosci.* **30**(32), 10639–10654 (2010). <https://doi.org/10.1523/JNEUROSCI.0059-10.2010>
 19. L.M. Machesky, Lamellipodia and filopodia in metastasis and invasion. *FEBS Lett.* **582**(14), 2102–2111 (2008). <https://doi.org/10.1016/j.febslet.2008.03.039>
 20. J.Y. Shih, S.C. Yang, T.M. Hong et al., Collapsin response mediator protein-1 and the invasion and metastasis of cancer cells. *J. Natl Cancer Inst.* **93**(18), 1392–1400 (2001). <https://doi.org/10.1093/jnci/93.18.1392>
 21. J.Y. Shih, Y.C. Lee, S.C. Yang et al., Collapsin response mediator protein-1: a novel invasion-suppressor gene. *Clin. Exp. Metastasis* **20**(1), 69–76 (2003). <https://doi.org/10.1023/a:1022598604565>
 22. C.C. Wu, J.C. Lin, S.C. Yang et al., Modulation of the expression of the invasion-suppressor CRMP-1 by cyclooxygenase-2 inhibition via reciprocal regulation of Sp1 and C/EBPalpha. *Mol. Cancer Ther.* **7**(6), 1365–1375 (2008). <https://doi.org/10.1158/1535-7163.MCT-08-0091>
 23. S.H. Pan, Y.C. Chao, P.F. Hung et al., The ability of LCRMP-1 to promote cancer invasion by enhancing filopodia formation is antagonized by CRMP-1. *J. Clin. Invest.* **121**(8), 3189–3205 (2011). <https://doi.org/10.1172/JCI42975>
 24. S.H. Pan, Y.C. Chao, H.Y. Chen et al., Long form collapsin response mediator protein-1 (LCRMP-1) expression is associated with clinical outcome and lymph node metastasis in non-small cell lung cancer patients. *Lung Cancer* **67**(1), 93–100 (2010). <https://doi.org/10.1016/j.lungcan.2009.03.006>
 25. W.L. Wang, T.M. Hong, Y.L. Chang et al., Phosphorylation of LCRMP-1 by GSK3beta promotes filopodia formation, migration and invasion abilities in lung cancer cells. *PLoS ONE* **7**(2), e31689(1-10) (2012). <https://doi.org/10.1371/journal.pone.0031689>
 26. E. Oliemuller, R. Pelaez, S. Garasa et al., Phosphorylated tubulin adaptor protein CRMP-2 as prognostic marker and candidate therapeutic target for NSCLC. *Int. J. Cancer* **132**(9), 1986–1995 (2013). <https://doi.org/10.1002/ijc.27881>
 27. C.C. Wu, H.C. Chen, S.J. Chen et al., Identification of collapsin response mediator protein-2 as a potential marker of colorectal carcinoma by comparative analysis of cancer cell secretomes. *Proteomics* **8**(2), 316–332 (2008). <https://doi.org/10.1002/pmic.200700819>
 28. M. Morgan-Fisher, Couchman JR., A. Yoneda, Phosphorylation and mRNA splicing of collapsin response mediator protein-2 determine inhibition of rho-associated protein kinase (ROCK) II function in carcinoma cell migration and invasion. *J. Biol. Chem.* **288**(43), 31229–31240 (2013). <https://doi.org/10.1074/jbc.M113.505602>
 29. E.E. Vincent, D.J. Elder, L. O'Flaherty et al., Glycogen synthase kinase 3 protein kinase activity is frequently elevated in human non-small cell lung carcinoma and supports tumour cell proliferation. *PLoS ONE* **9**(12), e114725(1–18) (2014). <https://doi.org/10.1371/journal.pone.0114725>
 30. Z. Yu, T.J. Kryzer, G.E. Griesmann et al., CRMP-5 neuronal autoantibody: marker of lung cancer and thymoma-related autoimmunity. *Ann. Neurol.* **49**(2), 146–154 (2001). [https://doi.org/10.1002/1531-8249\(20010201\)49:2%3c146:AID-ANA34%3e3.0.CO;2-E](https://doi.org/10.1002/1531-8249(20010201)49:2%3c146:AID-ANA34%3e3.0.CO;2-E)
 31. R. Sheorajpanday, H. Slabbynyck, W. Van De Sompel et al., Small cell lung carcinoma presenting as collapsin response-mediating protein (CRMP) -5 paraneoplastic optic neuropathy. *J. Neuroophthalmol.* **26**(3), 168–172 (2006). <https://doi.org/10.1097/OI.wno.0000235578.80051.0e>
 32. E. Margolin, A. Flint, J.D. Trobe, High-titer collapsin response-mediating protein-associated (CRMP-5) paraneoplastic optic neuropathy and Vitritis as the only clinical manifestations in a patient with small cell lung carcinoma. *J. Neuroophthalmol.* **28**(1), 17–22 (2008). <https://doi.org/10.1097/wno.0b013e3181675479>
 33. F.E.I. Liu, H.E. Youfeng, Z.H.I.F.U. Luo, Study of $^{99\text{m}}\text{Tc}$ labelled way analogues for 5-HT1A receptor imaging, IAEA, Technical Reports Series No. **426**, 37–45 (2004). https://inis.iaea.org/search/search.aspx?orig_q=RN:35080239
 34. K. Chakravarthy, D.G.D. Sankar, Development and validation of RP-HPLC method for estimation of lacosamide in bulk and its pharmaceutical formulation. *Rasayan J. Chem.* **4**(3), 666–672 (2011)

35. B.A. Rhodes, Considerations in the radiolabeling of albumin. *Sem. Nucl. Med.* **4**(3), 281–293 (1974). [https://doi.org/10.1016/S0001-2998\(74\)80015-2](https://doi.org/10.1016/S0001-2998(74)80015-2)
36. O.K. El-Kawy, H.T. Talaat, Preparation, characterization and evaluation of ^{186}Re -Idarubicin: a novel agent for diagnosis and treatment of hepatocellular carcinoma. *J. Label. Compd. Radiopharm.* **59**(2), 72–77 (2016). <https://doi.org/10.1002/jlcr.3368>
37. H.M. Talaat, M.I. Aydia, I.T. Ibrahim, H. El-Said, K.M. El-Azony, Preparation of ^{186}Re -Cefixime as a potential diagnostic and therapeutic agent for bacterial infection. *Egypt J. Radiat. Sci. Appl.* **32**(1), 95–103 (2019)
38. S.N.H. Azmi, B. Iqbal, N.S.H. Al-Humaimi et al., Quantitative analysis of cefixime via complexation with palladium(II) in pharmaceutical formulations by spectrophotometry. *J. Pharm. Anal.* **3**(4), 248–256 (2013). <https://doi.org/10.1016/j.jpha.2012.12.009>
39. O.W. Kolling, Reduction of perrhenate by stannous tin. *Trans. Kansas Acad. Sci.* **57**(4), 520–524 (1954). <https://doi.org/10.2307/3625940>
40. G.B. Saha, Fundamentals of nuclear pharmacy, 5th edition, Springer, chapter 6 “Radiopharmaceuticals and Methods”, pp. 99–109 (2003)
41. S. Shah, S.V. Vasantharaju, A. Karthik et al., Development and validation of stability-indicating assay method for lacosamide by RP- HPLC. *Elixir. Inter. J. Pharm.* **38**, 4174–4177 (2011)
42. S. De Biase, M. Valente, G.L. Gigli et al., Pharmacokinetic drug evaluation of lacosamide for the treatment of partial-onset seizures. *Expert Opin. Drug Metab. Toxicol.* **13**(9), 997–1005 (2017). <https://doi.org/10.1080/17425255.2017.1360278>
43. M.H. Wong, N.B. Fountain, Lacosamide for the treatment of partial-onset seizures. *Therapy* **7**(5), 459–465 (2010)
44. R.C. Walovitch, T.C. Hill, S.T. Garrity et al., Characterization of technetium-99 m-L, L-ECD for brain perfusion imaging, part 1: pharmacology of technetium-99 m ECD in nonhuman primates. *J. Nucl. Med.* **30**, 1892–1901 (1989)
45. R.D. Neirinckx, I.R. Canning, I.M. Piper et al., Technetium-99 m d, l-HM-PAO: a new rathopharmaceutical for SPECT imaging of regional cerebralblood perfusion. *J. Nucl. Med.* **28**, 191–202 (1987)
46. H.A. El-Sabagh, H.M. Talaat, M.S. Abdel-Mottaleb, Preparation and biodistribution of ^{99m}Tc -trazodone as a brain imaging probe. *J. Radiochem.* **61**(1), 93–98 (2019). <https://doi.org/10.1134/S1066362219010144>
47. M.A. Motaleb, I.T. Ibrahim, V.R. Ayoub et al., Preparation and biological evaluation of (99m)Tc-ropinirole as a novel radiopharmaceutical for brain imaging. *J. Label Comp. Radiopharm.* **59**(4), 147–152 (2016). <https://doi.org/10.1002/jlcr.3380>
48. A.M. Amin, K.M. El-Azony, I.T. Ibrahim, Application of $^{99}\text{Mo}/^{99m}\text{Tc}$ alumina generator in the labeling of metoprolol for diagnostic purposes. *J. Label Compd. Radiopharm.* **52**(11), 467–472 (2009). <https://doi.org/10.1002/jlcr.1661>
49. Y. Wang, J.M. Brittain, B.W. Jarecki et al., In silico docking and electrophysiological characterization of lacosamide binding sites on collapsin response mediator protein-2 identifies a pocket important in modulating sodium channel slow inactivation. *J. Biol. Chem.* **285**(33), 25296–25307 (2010). <https://doi.org/10.1074/jbc.M110.128801>